Tectonics®

RESEARCH ARTICLE
10.1029/2021TC006990

Key Points:

- South Georgia is a microcontinent on the Scotia Ridge regarded as a continuation of the Andes. To test this, oriented samples were collected
- The paleomagnetic results agree with studies from the Andes supporting the paleoposition of the South Georgia indicated by the geology
- Partitioning this rotation between oroclinal bending and translation along the North Scotia Ridge is not possible on paleomagnetic grounds

Supporting Information:

Supporting Information may be found in the online version of this article.

Correspondence to:

I. W. D. Dalziel,
ian@ig.utexas.edu

Citation:

Beaver, D. G., Kent, D. V., & Dalziel, I. W. D. (2022). Paleomagnetic constraints from South Georgia on the tectonic reconstruction of the Early Cretaceous Rocas Verdes marginal basin system of southernmost South America. *Tectonics*, *41*, e2021TC006990. https://doi.org/10.1029/2021TC006990

Received 25 JUL 2021
Accepted 16 JAN 2022

Author Contributions:

Conceptualization: Ian W. D. Dalziel
Data curation: Douglas G. Beaver, Dennis V. Kent
Formal analysis: Douglas G. Beaver, Dennis V. Kent
Funding acquisition: Ian W. D. Dalziel
Investigation: Douglas G. Beaver, Dennis V. Kent, Ian W. D. Dalziel
Project Administration: Ian W. D. Dalziel
Resources: Dennis V. Kent
Supervision: Ian W. D. Dalziel
Writing – original draft: Douglas G. Beaver, Dennis V. Kent, Ian W. D. Dalziel
Writing – review & editing: Douglas G. Beaver, Dennis V. Kent, Ian W. D. Dalziel

Paleomagnetic Constraints From South Georgia on the Tectonic Reconstruction of the Early Cretaceous Rocas Verdes Marginal Basin System of Southernmost South America

Douglas G. Beaver[1], Dennis V. Kent[2,3], and Ian W. D. Dalziel[4]

[1]Rare Earth Environsciences, Inc., Harleysville, PA, USA, [2]Lamont-Doherty Earth Observatory of Columbia University, Palisades, NY, USA, [3]Earth & Planetary Sciences, Rutgers University, Piscataway, NJ, USA, [4]Institute for Geophysics, Jackson School of Geosciences, The University of Texas at Austin, Austin, TX, USA

Abstract South Georgia exists as a microcontinent along the North Scotia Ridge ~1,700 km east of Cape Horn. The tectonostratigraphic units of South Georgia have long been correlated with those of the Fuegian Andes of southernmost South America. Accordingly, South Georgia has been regarded as a continuation of the Late Jurassic–Early Cretaceous Rocas Verdes marginal basin system, formerly situated south of Burdwood Bank and east of Cape Horn. To test this, paleomagnetic analysis of samples from the Larsen Harbour Complex, Drygalski Fjord Complex, and Annenkov Island Formation of South Georgia showed that 21 sites yield a mean direction of D = 328.5°, I = −62.1° (a95 = 3.5°) and a paleomagnetic pole at 068.2°E, 67.2°N, A95 = 4.7°. The consistency of directions and strong polarity bias, plus indications of a negative differential tilt test, point to a secondary magnetization acquired in the Late Cretaceous. Comparison of predicted versus observed directions for South Georgia relative to stable South America indicate 27.2 ± 11.2° of counter-clockwise rotation (and 10.5° ± 4.5° of northward tilting) since the acquisition of magnetization. These results are consistent with paleomagnetic studies from the Fuegian Andes and support a paleoposition of the South Georgia microcontinent south of Burdwood Bank as strongly indicated by the geologic evidence. Partitioning this rotation between oroclinal bending during the Rocas Verdes basin collapse in the Late Cretaceous and left-lateral translation along the North Scotia Ridge is not possible on paleomagnetic grounds, but the co-linearity of Andean structures between the restored microcontinent and Tierra del Fuego indicates the former.

Plain Language Summary The South Atlantic island of South Georgia forms the mountainous, glaciated, core of a microcontinent. Located some 1,700 km east of Cape Horn at the southern tip of South America, it is one of the most isolated fragments of continental crust on Earth. For many decades geological evidence has been accumulating that points to the island and hence the entire microcontinent being a displaced fragment of the Andean Cordillera of Tierra del Fuego. To test this hypothesis we collected oriented samples from igneous rocks on the main and offshore islands. The results are directly comparable to those obtained from samples from Tierra del Fuego and therefore support the geological evidence that the microcontinent originated as a continuation of the Andean Cordillera and was displaced eastward relative to South America during the opening of the South Atlantic Ocean basin.

1. Introduction

From the Arica embayment at 18°30'S the Andean Cordillera trends almost due south for some 4,000 km to the west end of the Strait of Magellan (Figure 1). There, at ~53°S, it swings eastward through the Patagonian orocline (Carey, 1955) to plunge into the South Atlantic Ocean at the eastern extremity of Isla de los Estados and continue eastward at ~54° 30'S as the mainly submerged North Scotia Ridge (Bruce, 1905). The ridge terminates some 1,700 km east of Isla de los Estados in a microcontinent emergent as the mountainous, glaciated island of South Georgia. This is one of the most isolated continental fragments on Earth.

The geological character of the South Georgia microcontinent (SGM) is in direct contrast to its current position, isolated by oceanic crust and lacking a feasible provenance for some of its major metasedimentary constituents. The geologic similarities between the SGM and the southernmost Andes prompted early workers to postulate a much closer geographic relationship between the two (Hawkes, 1962; Matthews, 1959). Subsequent analyses provide strong geological evidence that the SGM is a fragment of the Andean Cordillera detached from its hinterland in southeastern Tierra del Fuego (Dalziel et al., 1975, 2021). These reconstructions predict a paleo-tectonic

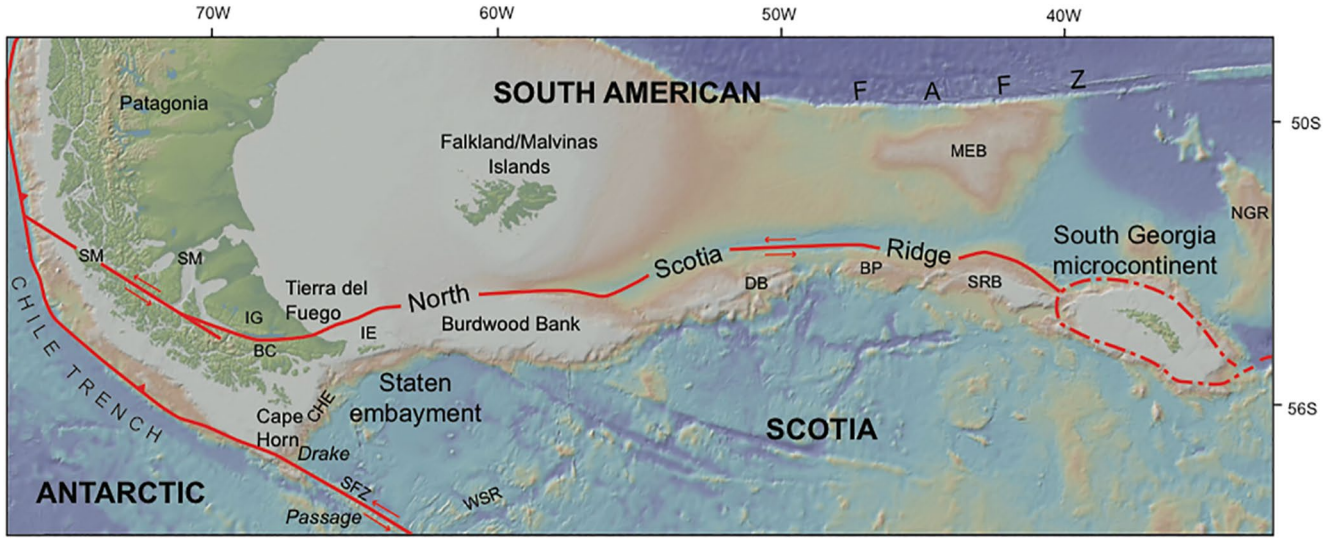

Figure 1. Generalized geographic setting of the South Georgia microcontinent in relation to the Antarctic, South American and Scotia plates (GeoMapApp). Plate boundaries are shown in red with "teeth" on the upper plate of the Antarctic-South American subduction zone and arrows showing relative motion along the South American-Scotia and Antarctic-Scotia transform boundaries. BC, Beagle Channel; BP, Barker Plateau; CHE, Cape Horn escarpment; DB, Davis Bank; FAFZ, Falkland-Agulhas Fracture Zone; IE, Isla de los Estados; IG, Isla Grande; MEB, Maurice Ewing Bank; NGR, Northeast Georgia Rise; SFZ, Shackleton Fracture Zone; SM, Strait of Magellan; SRB, Shag Rocks Bank; WSR, West Scotia Ridge.

position immediately east of Cape Horn and due south of Isla de los Estados and Burdwood Bank, which we take to be our null hypothesis; however, other plate reconstruction models resulting from study of geophysical data from the South Atlantic Ocean, the Scotia Sea and the Weddell Sea would place the SGM off Maurice Ewing Bank much farther to the east (Eagles, 2010b; Eagles & Eisermann, 2020). Constraining the initial position of the SGM is important for understanding the paleogeography of this southern margin of the South American continent as it evolved during the late Mesozoic and Cenozoic, playing a critical role in the onset and development of the Antarctic Circumpolar Current (Carter et al., 2014; Dalziel, Lawver, Norton, et al., 2013; Dalziel, Lawver, Pearce, et al., 2013) and hence influencing global climate.

During May and June of 1985, two contributors (Beaver and Dalziel) sailed to South Georgia on the inaugural austral winter research cruise of RV *Polar Duke* as participants in the "Tectonics of the Scotia Arc" project of Lamont-Doherty Geological (now Earth) Observatory of Columbia University, part of the United States Antarctic Research Program (now *sans* "Research"). The objective of the research voyage was to obtain samples for radiometric dating and paleomagnetic study. The geochronometry was published (Mukasa & Dalziel, 1996) and is discussed below. Although the paleomagnetic samples were processed in the Paleomagnetics Laboratory at Lamont and the results written up and submitted for publication in 1989 and even accepted subject to revision, that revision, for various personal reasons, was never undertaken. Here we update the manuscript in response to journal reviewers' comments and interpret the paleomagnetic data in the light of modern paleomagnetic reference poles for stable South America and data from the tectonically rotated hinterland of the Fuegian Andes, as revealed in previous and more recent paleomagnetic studies (Burns et al., 1980; Dalziel et al., 1973; Poblete et al., 2016; Rapalini et al., 2016), and in conjunction with our current understanding of the geology of the SGM as recently reviewed by (Dalziel et al., 2021). To our knowledge, this remains the only paleomagnetic study conducted on South Georgia.

2. Tectonic Setting

2.1. Rocas Verdes Marginal Basin

The key to understanding the tectonic evolution of the southernmost Andean Cordillera in Patagonia and Tierra del Fuego is the Rocas Verdes ("Green Rocks") basin (Dalziel, de Wit, & Palmer, 1974; Katz, 1964, 1972; Figure 2). This is the southernmost of a "string" of extensional basins that opened along the Andean continental margin of South America during the Late Jurassic to Early Cretaceous (Dalziel, 1986). It opened following a

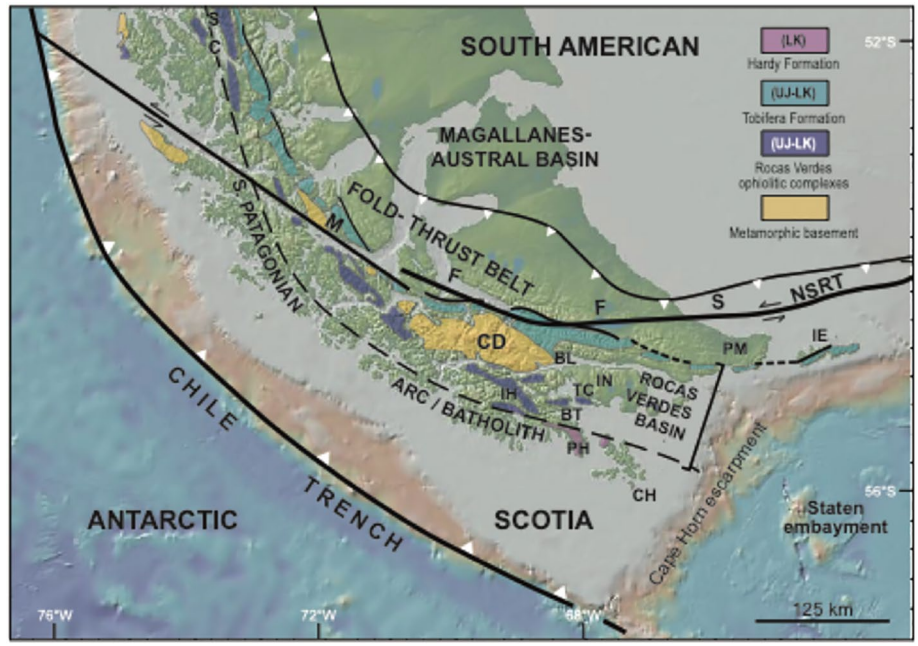

Figure 2. Simplified geologic map of the southernmost Andes (GeoMappApp; Dalziel et al., 2021) showing Antarctic, Scotia and South American plates. The uncolored areas within the Rocas Verdes basin are underlain by the Lower Cretaceous Yahgan Formation. BL, Bahia Lapataia; BT, Bahia Tekenika; CD, Cordillera Darwin; CH, Cape Horn; IE, Isla de los Estados; IH, Isla Hoste; IN, Isla Navarino; MFFS, Magallanes-Fagnano fault system; NSRT, North Scotia Ridge transform; PH, Peninsula Hardy; SC, Sarmiento Complex; TC, Tortuga Complex.

widespread rifting event accompanied by the extrusion of dominantly silicic volcanics known as the Tobifera Formation in Chile and the Lemaire Formation in Argentina (Bruhn et al., 1978) and is floored by extended continental basement and quasi-oceanic to oceanic crust now preserved as ophiolitic complexes (Calderón et al., 2013; Dalziel, de Wit, & Palmer, 1974; Stern & de Wit, 2003). The basin is bordered on its Pacific side by a sliver of continental basement hosting the south Patagonian and Fuegian arc and underlying batholith. After formation of the oceanic floor of the basin in the Late Jurassic (Hervé et al., 2007; Stern et al., 1992), detritus from arc activity filled the basin during the Early Cretaceous forming the turbiditic Yahgan Formation (Dott et al., 1982; Katz & Watters, 1966).

The rock units of the Rocas Verdes and Fuegian arc/batholith terminate abruptly at the Cape Horn escarpment, while the Tobifera/Lemaire Formation continues eastward through Isla de los Estados and along the southern margin of the submerged Burdwood Bank (Dalziel, Caminos, et al., 1974); this leaves an embayment in the southeastern tip of South American continental margin, the Staten embayment (Dalziel et al., 2021; Figure 2). The rocks forming the island of South Georgia and offshore islets exactly match the units truncated at the Cape Horn escarpment and missing in the Staten embayment. The history of more than a century of multi-national geologic studies on South Georgia and of growing appreciation of its affinities with the southernmost Andes is outlined in the review article of Dalziel et al. (2021). Most of the main island is formed by turbidites of the Cumberland Bay and Sandebugten formations (Figure 3) that can be correlated in age and sedimentologic characteristics to the Yahgan and other sedimentary formations of Tierra del Fuego (Figure 4). The turbidites filled in a basin floored by stretched continental crust, the Drygalski Complex (Storey, 1983), and Late Jurassic oceanic crust, the Larsen Harbour Complex (Mair, 1987), fringed on the Pacific side by island arc rocks of the Annenkov Island Formation (Suarez & Pettigrew, 1976; Tanner et al., 1981). There is thus a close correlation with the rocks of the Fuegian Andes (Dalziel et al., 2021). Moreover, the provenance of the turbidites on South Georgia can be closely matched with sources in Tierra del Fuego that are absent in the island's present location and differ markedly from those to be expected in the more easterly original location implied by the plate reconstruction models of Eagles (2010a) and Eagles and Eisermann (2020) (Carter et al., 2014; Dalziel et al., 1975; see further discussion in Dalziel et al., 2021).

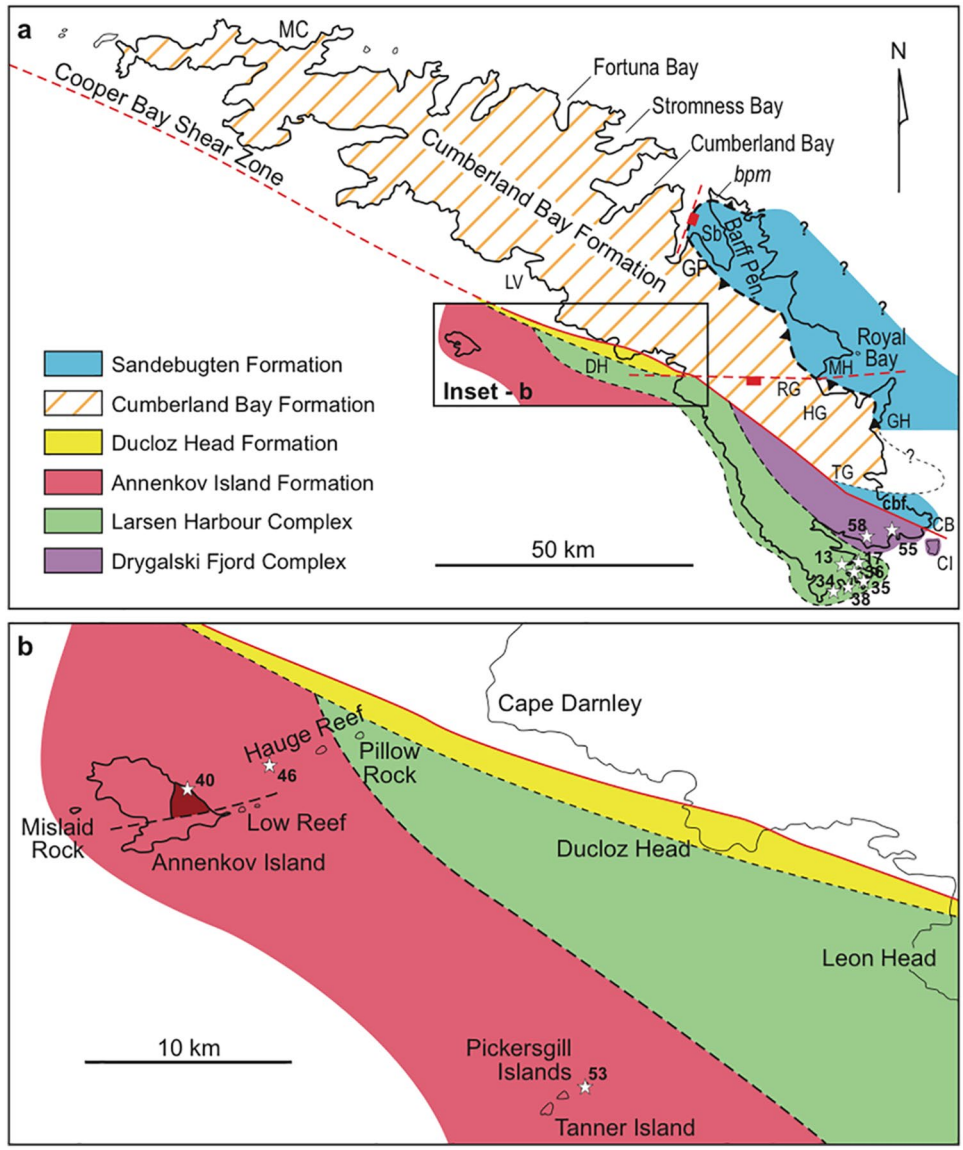

Figure 3. Simplified geologic maps of South Georgia and offshore islands (Dalziel et al., 2021) delineating tectonostratigraphic subdivisions and showing paleomagnetic sampling sites (see Figures S1–S3 in Supporting Information S1 for more details).

2.2. The Patagonian Orocline

The Rocas Verdes basin remained open, receiving sedimentary detritus mainly from the Pacific margin volcanic arc, through most of the Early Cretaceous. Sedimentation of the Cumberland Bay Formation is believed to have ceased before the start of the Turonian Stage of the Late Cretaceous at ca. 100 Ma (Dalziel et al., 2021). Late Cretaceous post-tectonic plutons of the Beagle granite suite in Tierra del Fuego intrude folded Yahgan Formation strata, reflecting continent-ward displacement of the locus of arc activity (Klepeis et al., 2010; Mukasa & Dalziel, 1996). This relationship of post-tectonic plutons cutting deformed Lower Cretaceous marginal basin strata continues north along the Andes at least as far as the West Peruvian trough and may reflect accelerated western motion of the South America plate and continent in a mantle reference frame (Dalziel, 1986; Horton & Fuentes, 2016). Mid-Cretaceous to early Late Cretaceous initiation of deformation, closure and inversion of the Rocas Verdes also correlates with the timing of flexural down-warp of the Magallanes-Austral foredeep basin (Natland et al., 1974; Figure 1).

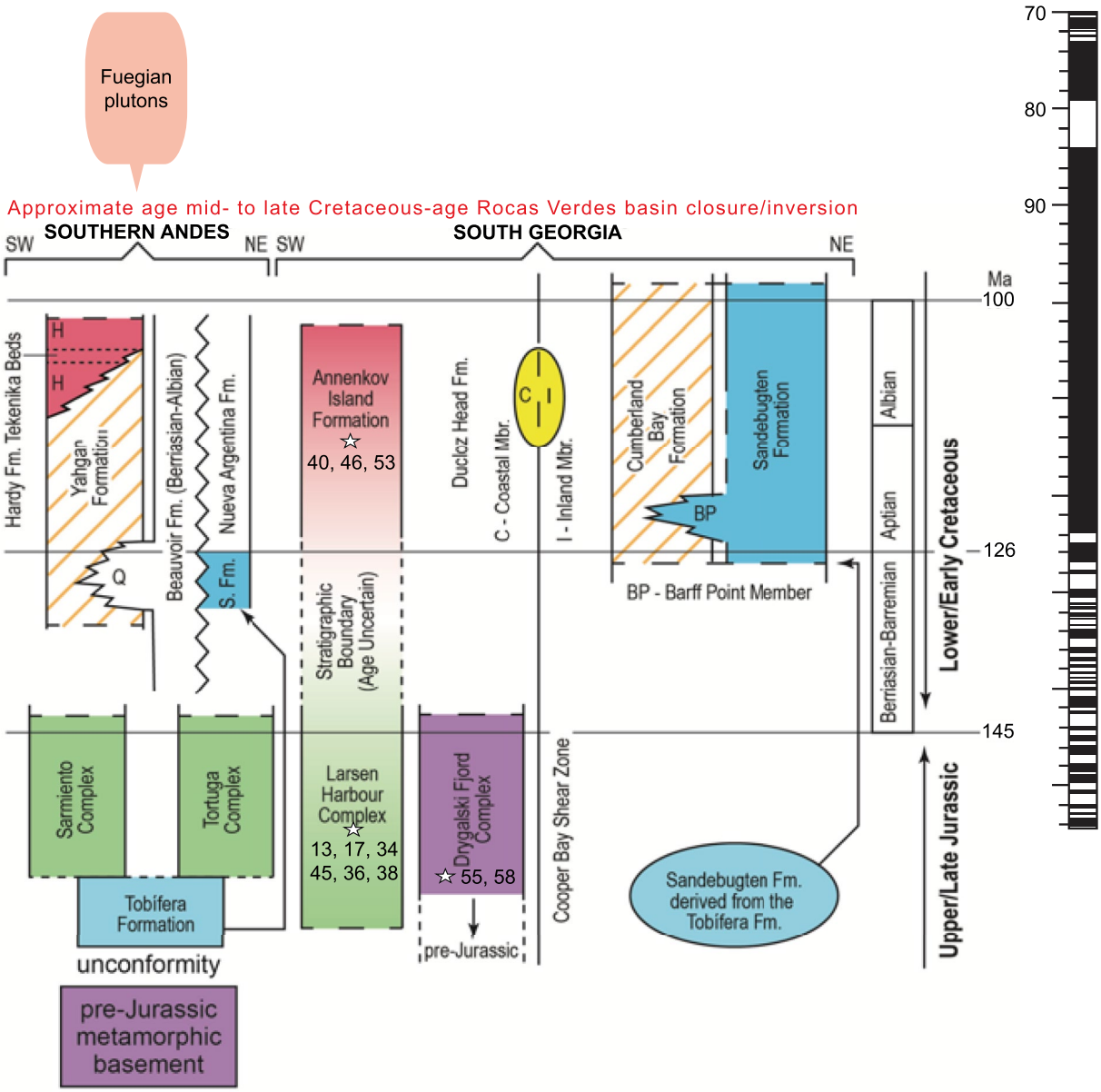

Figure 4. Tectonostratigraphic columns for South Georgia compared to Fuegian Andes (Dalziel et al., 2021) showing approximate stratigraphic positions of sampling sites, timing of Rocas Verdes closure/inversion, and approximate age of Fuegian plutons. The colors correspond to those on the geologic maps of South Georgia (Figure 3). Geomagnetic polarity time scale (filled/open bars denote normal/reverse polarity) (Gradstein et al., 2012) shown for reference.

The trend of structures in the inverted Rocas Verdes basin follows the continental margin and the Andean Cordillera around the Patagonian orocline from north-south, to the north of the Strait of Magellan, to easterly in Tierra del Fuego. Alignment of the prominent folds that run the length of South Georgia permits palinspastic restoration of the SGM in the Staten embayment compatible with continuation of the Fuegian arc and batholith into the present southwestern side of the microcontinent (Dalziel et al., 2021), as will be argued below.

All of the aforementioned elements point to the cogenetic evolution of the southernmost Andes and South Georgia and suggest that this microcontinent is an eastward continuation of the Rocas Verdes marginal basin system displaced from its paleo-tectonic position south of Burdwood Bank. This supposition can be tested by comparing the paleomagnetic evidence for oroclinal rotations in the southernmost Andes (Burns et al., 1980; Dalziel et al., 1973; Poblete et al., 2014, 2016; Rapalini, 2007; Rapalini et al., 2016) with our new results from South Georgia described below.

3. Sampling

As a consequence of weather and sea conditions and the scope of project, sampling was restricted to three tectonostratigraphic units: the Larsen Harbour Complex, Drygalski Fjord Complex, and the Annenkov Island Formation (Figure 3 and Figure S1 in Supporting Information S1). Samples were collected using a portable gasoline-powered coring drill and oriented by magnetic compass taking into account the local declination variation estimated from navigation charts (−8.1° for the Larsen Harbour and Drygalski Fjord complexes, −7.7° for the Annenkov Island Formation). The hierarchy of sampling is as follows: a locality was considered to be a location of geographic distinction; a site, an outcrop; and a sample, a geologically representative, independently oriented core at an associated site. In keeping with standard paleomagnetic sampling practice a minimum of six cores were collected at each site. A total of thirteen localities were visited and 28 sites sampled each with a minimum of six oriented cores, with the exceptions of SG17B and SG17D which had five samples collected and SG58B which had four samples collected.

The Larsen Harbour Complex (Figures 3 and Figure S2 in Supporting Information S1) is characterized by thick sequences of basic pillow lavas, stratified breccias, and volcanogenic sediments interbedded with radiolarian sediments and minor felsic (rhyolitic) extrusions and basic dikes, overlain by the areally extensive Cumberland Bay Formation. Concordant U-Pb analyses of zircons from the gabbro and plagiogranite phases of the ophiolitic complex at Smaaland Cove indicate an age of approximately 150 Ma (Mukasa & Dalziel, 1996), whereas the Cumberland Bay Formation has yielded belemnites of Late Jurassic to Early Cretaceous age (Stone & Willey, 1973). Metamorphism of the complex ranges from prehnite-pumpellyite to greenschist facies depending upon the level of exposure (Mair, 1983, 1987). A diverse lithologic range of samples was collected from 14 sites in the Larsen Harbour Complex, consisting of nine mafic dikes of Doubtful Bay, Smaaland Cove, and Larsen Harbour as well as three pillow lavas, a volcaniclastic turbidite and a breccia from Larsen Harbour (Figure 3 and Figure S2 in Supporting Information S1; Table 1). The only structural control in the Larsen Harbour Complex was provided by the pillow lavas (SG13A, SG17B, SG17C) and a volcanoclastic unit (SG13B), which were dipping 36°SW about a strike of 160° (Table 2).

The Drygalski Fjord Complex is situated immediately to the northeast of the Larsen Harbour Complex. The predominant igneous component of the Drygalski Fjord Complex is gabbroic (Storey & Mair, 1982). Dating of hornblendes from these gabbros by K-Ar and Rb-Sr analysis of an isolated felsic body, the Trendall Crag Granite, yield ages of 186 ± 9 Ma to 201 ± 7 Ma and 181 ± 30 Ma, respectively (Tanner & Rex, 1979). The Drygalski Fjord Complex was sampled at five sites (Figures 3 and Figure S3 in Supporting Information S1; Table 1). Two sites were sampled along the western side of the eastern headland of Hamilton Bay in subvertically layered gabbros (SG55A, SG55B). Three sites, all mafic dikes (SG3A, SG58A, and SG58B), were located along the eastern wall of Drygalski Fjord. None of the Drygalski Fjord Complex sites had a reliable reference frame to determine paleo-horizontal.

To the southwest of South Georgia lie the smaller islands of Annenkov, Hauge Reef and the Pickersgills (Figure 3b and Figure S3 in Supporting Information S1). The predominant lithologies are metasediments of zeolite facies divisible into two units, the Lower Tuff and Upper Breccia members (Pettigrew, 1981; Suarez & Pettigrew, 1976). Both members are virtually undeformed, lack a tectonically imposed fabric and have bedding tilts on the order of 20° to the southwest and northwest. The Lower Tuff member is composed of regularly interbedded tuffs and tuffaceous mudstones with a calc-alkaline provenance. This unit is highly fossiliferous and has yielded ammonites of Neocomian to Aptian age (Pettigrew, 1981). Conformably overlying this unit is the Upper Breccia member, an alternation of poorly sorted coarse andesitic breccias and subordinate sandstones likewise of andesitic provenance (Pettigrew, 1981) with a Late Aptian-Albian age based on the occurrence of fossil belemnites (Pettigrew & Willey, 1975). Rb-Sr analysis of a large monzodioritic pluton of the Pickersgills Islands indicates a Late Cretaceous age of 81 ± 10 Ma, which is compatible with the fossil ages of the intruded sedimentary units (Tanner & Rex, 1979). The sampling of the Annenkov Island Formation at five sites (Table 1) was restricted to the Lower Tuff member and consisted of two sites in metasediments on the northeastern coast of Annenkov Island, two sites in metasediments and one site in a pillow lava on the southwest coast of Island A of Hauge Reef. Two sites in diorites (SG51A and SG51B) were also collected from the most southwesterly island in the Pickersgill chain, Tanner Island, and two sites in gabbros (SG53A and SG53B) were collected from the most northeasterly island (Figures 3b and 4). Bedding tilt could be determined for the four sites of the Lower Tuff Member (SG40A and SG40B: 20°NW about astrike of 235°; SG46B and SG46C: 18°SW about a strike of 120°) and the sole pillow lava site on Island A (SG46A: 5°SW about a strike of 120°; Table 2).

Table 1
Site Mean Paleomagnetic Directions for South Georgia Sites

SITE	sLAT (°S)	sLON (°W)	*n*	*k*	a95 (°)	gDEC (°)	gINC (°)	pLON (°E)	pLAT (°N)	LITHOLOGY
Larsen Harbour Complex										
SG13A	54.84	36.03	9	102	5.1	347.7	−62.0	284.3	75.9	Pillow lava
SG13B	54.86	36.01	0							Volcaniclastic
SG13C	54.84	36.02	0							Breccia
SG17A	54.83	36.00	5	533	3.2	342.7	−71.9	215.1	80.2	Mafic dike
SG17B	54.84	36.12	0							Pillow lava
SG17C	54.86	36.00	0							Pillow lava
SG17D	54.83	36.00	4	50	13.2	315.5	−62.5	236.4	59.6	Mafic dike
SG17E	54.83	36.00	6	212	4.6	323.4	−55.9	255.1	59.1	Mafic dike
SG34A	54.88	36.04	6	564	2.8	313.2	−58.3	241.0	55.3	Mafic dike
SG34B	54.88	36.04	6	481	3.2	318.1	−64.0	235.5	62.2	Mafic dike
SG35A	54.87	36.00	6	73	7.9	322.4	−63.8	239.8	64.5	Mafic dike
SG35B	54.87	36.00	6	376	3.5	329.9	−71.3	217.9	73.0	Mafic dike
SG36A	54.87	36.00	6	146	5.6	325.0	−68.3	228.5	69.0	Mafic dike
SG38A	54.88	36.01	3	105	12.1	322.7	−65.3	236.2	65.8	Mafic dike
Mean	54.9	36.0	10	133	4.2	325.2	−64.7	239.5	67.2	
									(A95 = 6.1°)	
Annenkov Island Group										
SG40A	54.49	37.04	6	902	2.2	342.2	−51.4	286.4	64.3	Metasediment
SG40B	54.49	37.04	6	202	4.7	334.1	−50.9	273.7	60.6	Metasediment
SG46A	54.47	36.98	5	75	8.9	353.2	−74.4	170.1	82.7	Pillow lava
SG46B	54.47	36.98	5	190	5.6	336.5	−65.8	247.2	74.0	Metasediment
SG46C	54.47	36.98	5	639	3.0	325.9	−65.9	235.6	68.0	Metasediment
SG51A	54.47	36.98	0							Diorite
SG51B	54.48	36.98	0							Diorite
SG53A	54.63	36.74	6	1297	1.9	316.9	−64.4	232.0	61.8	Gabbro
SG53B	54.63	36.74	6	161	5.3	310.9	−63.8	228.7	57.9	Gabbro
Mean	54.5	36.9	7	60	7.8	331.1	−62.9	247.2	69.3	
									(A95 = 10.6°)	
Drygalski Fjord Complex										
SG55A	54.80	35.89	6	235	4.4	339.8	−56.3	278.1	67.4	Gabbro
SG55B	54.80	35.89	6	300	3.9	334.2	−53.3	272.7	62.4	Gabbro
SG58A	54.80	35.99	6	222	4.5	327.4	−53.1	263.5	59.0	Mafic dike
SG58B	54.80	35.99	2	377	12.9	323.9	−52.6	259.7	56.8	Mafic dike
SG3A	54.79	36.04	0							Mafic dike
Mean	54.8	35.9	4	329	5.1	331.1	−54.0	267.6	61.6	
									(A95 = 6.9°)	

Table 1
Continued

SITE	sLAT (°S)	sLON (°W)	*n*	*k*	a95 (°)	gDEC (°)	gINC (°)	pLON (°E)	pLAT (°N)	LITHOLOGY
All Sites										
Mean	54.7	36.3	21	86	3.5	328.5	−62.1	248.2	67.2 (A95 = 4.7°)	

Note. SITE, paleomagnetic sampling site; sLAT and sLON, latitude and longitude of sampling site; *n*, number of samples providing acceptable demagnetization trajectory (number of sites for GRAND MEAN); k, estimate of Fisher's precision parameter; a95, radius of circle of 95% confidence; gDEC and gINC, declination and inclination of site mean direction in geographic coordinates; pLON and pLAT, longitude and latitude of virtual geomagnetic north pole corresponding to site mean direction in geographic coordinates; LITHOLOGY, dominant lithology of sampled rock unit. Mean paleolatitude for center of sampling locations (54.7°S 36.3°W) is 43.3° ± 4.7°S.

The geologic setting and relative ages of the samples used in the study are shown in Figure 4 on a diagram correlating the tectonostratigraphic units of the SGM with those in Tierra del Fuego.

4. Laboratory Study

4.1. Procedures

Individually oriented 2.5-cm-diameter cores were prepared for analysis by slicing them into two or more specimens 2.2 cm in length for measurements and analyses. Two representative specimens from each site were chosen as pilots for progressive thermal (TD) and alternating field (AF) demagnetization using a Schonstedt TSD-1 thermal specimen demagnetizer and Schonstedt GSD-1 AC specimen demagnetizer, respectively. The natural remanent magnetization (NRM) before and after each demagnetization step was measured either with a Digico fluxgate spinner magnetometer (Molyneux, 1971) or a ScT two-axis cryogenic magnetometer (Goree & Fuller, 1976).

Based upon the analysis of the pilot specimen demagnetizations utilizing vector end-point diagrams (Zijderveld, 1967), remaining specimens from each site were progressively demagnetized either by AF or TD, whichever method proved to be more effective in revealing relevant magnetization components. All specimens were subjected to a minimum of six demagnetization steps. Demagnetization was considered complete when individual specimens achieved a linear trajectory tending toward the origin and/or had their remanent intensities reduced to less than 5% of their initial NRM values. A linear trajectory was estimated from three or more (typically six or more) consecutive demagnetization steps using principal component analysis; MAD values (Kirschvink, 1980) were typically less than 5° with only a handful of samples ranging higher to a maximum of 13°; site, locality and overall mean directions were calculated using Fisher statistics (Fisher, 1953).

4.2. Results

4.2.1. Larsen Harbour Complex

Remanent intensities of sites sampled within the Larsen Harbour Complex range widely, from about 1 mA/m to 10 A/m, with the pillow lavas representing the lower end of this range and the mafic dikes more variable. Linear demagnetization trajectories are well defined in all nine of the mafic dike sites and sample response to both AF and thermal demagnetization within sites was not notably dissimilar (Figure 5a); maximum unblocking temperatures typically are just below 600°C, consistent with magnetite as the principal magnetic carrier. The dominant stable direction is toward the northwest with moderately steep upward inclination.

The three pillow lavas sampled within the Larsen Harbour Complex (SG13A, SG17B and SG17C) did not produce as consistent results. One pillow lava (SG13A) possessing remanent intensities of 1 A/m yields final demagnetization trajectories compatible with the established directions in the mafic dikes, northwesterly and steeply up (Figure 5b). Of the two remaining pillows, one site (SG17B) yielded errant trajectories whereas weakly magnetized samples from site SG17C exhibit what appears to be a vestige of a reverse polarity component (southwesterly and down) after removal of a northerly and up overprint (Figure 5c).

For samples from a volcanic breccia (SG13C) and a volcaniclastite (SG13B), AF demagnetization yields a component comparable to the dominant direction of the Larsen Harbour Complex (northwesterly and up) whereas

Table 2
Site Mean Directions for Differential Tilt Test

SITE	DIP	STK	*n*	k	a95 (°)	gDEC (°)	gINC (°)	bDEC (°)	bINC (°)	LITHOLOGY
SG13A	36	160	9	102	5.1	347.7	−62.0	30.8	−42.6	Pillow lava
SG40A	20	235	6	902	2.2	342.2	−51.4	357.2	−69.8	Metasediment
SG40B	20	235	6	202	4.7	334.1	−50.9	342.3	−70.4	Metasediment
SG46A	5	120	5	75	8.9	353.2	−74.4	1.6	−70.2	Pillow lava
SG46B	18	120	5	190	5.6	336.5	−65.8	357.3	−52.4	Metasediment
SG46C	18	120	5	639	3.0	325.9	−65.9	350.9	−54.4	Metasediment
Tilt Test Results										
Geographic										
			6	65.2	8.4	339.2	−62.0			
Tilt Corrected										
			6	29.9	12.5			3.0	−61.0	

Note. SITE, paleomagnetic sampling site (see Table 1 for location); bedding orientation where bedding dip (DIP) is 90° clockwise from strike (STK). *n* is number of samples (number of sites for overall means); k is Fisher's precision parameter; a95 is radius of circle of 95% confidence about the mean direction; gDEC and gINC are the mean declination and inclination in geographic coordinates; bDEC and bINC are the mean declination and inclination after bedding tilt correction; LITHOLOGY is dominant rock type.

thermal demagnetization reveals noisy demagnetization trajectories with an irresolvable high unblocking temperature component. Consequently, these two sites have been rejected from further consideration.

Site mean directions in geographic coordinates for the 10 accepted sites from the Larsen Harbour Complex are listed in Table 1 and plotted in an equal-area projection in Figure 6a, where they are seen to cluster in the northwest quadrant with a steep negative inclination (D/I = 325.2°/−64.7°, a95 = 4.2°). The one site with structural control yielding reliable results (SG13A) is discussed below in the context of an overall differential tilt test.

4.2.2. Drygalski Fjord Complex

Three mafic dikes and two sites within a layered gabbro were sampled from the Drygalski Fjord Complex. Remanent intensities of these units are variable on the order of 0.01–1 A/M. Two of the mafic dikes, sites SG58A and SG58B, revealed only a northerly and shallow magnetization with AF demagnetization whereas progressive thermal demagnetization produced a univectorial component in the northwest quadrant and of moderate negative inclination after removal of a spurious low unblocking temperature component. Progressive AF or thermal demagnetization did not define a coherent component trajectory for the third mafic dike (SG3A) which was thus excluded from further analysis.

Demagnetization of the gabbros was effectively accomplished in either AF or thermal fields with differing results. Thermal demagnetization produced a univectorial component of maximum unblocking temperatures between 570 and 580°C, indicating magnetite as the dominant magnetic phase (Figure 5d). The response to AF demagnetization was notably dissimilar in that there was the elucidation of two distinct magnetization components (Figure 5e). These components, seen in six of seven samples of site SG55A subjected to AF demagnetization, are: (1) a lower coercivity (to 60 mT) component of moderate negative inclination to the northwest; and (2) a higher coercivity component of somewhat steeper negative inclination and directed more northerly. The lower coercivity northwest component more closely parallels the magnetization direction found in thermal demagnetization of the gabbros (e.g., Figure 5d) as well as in most of the other rocks studied from South Georgia. The higher coercivity component in the gabbros resembles the present-day field direction but is poorly revealed in thermal demagnetization. We regard the well-developed lower coercivity northwest and up component also isolated by thermal demagnetization as the characteristic magnetization.

Site mean directions of the Drygalski Fjord Complex in geographic coordinates are listed in Table 1 and plotted in Figure 6b. Consistent with the established characteristic direction of South Georgia the site mean direction for the four accepted sites is NNW and up (D/I = 331.1°/−54.0°, a95 = 5.1°); however, lack of structural control at any of the sampled sites precludes including them in an overall differential tilt test.

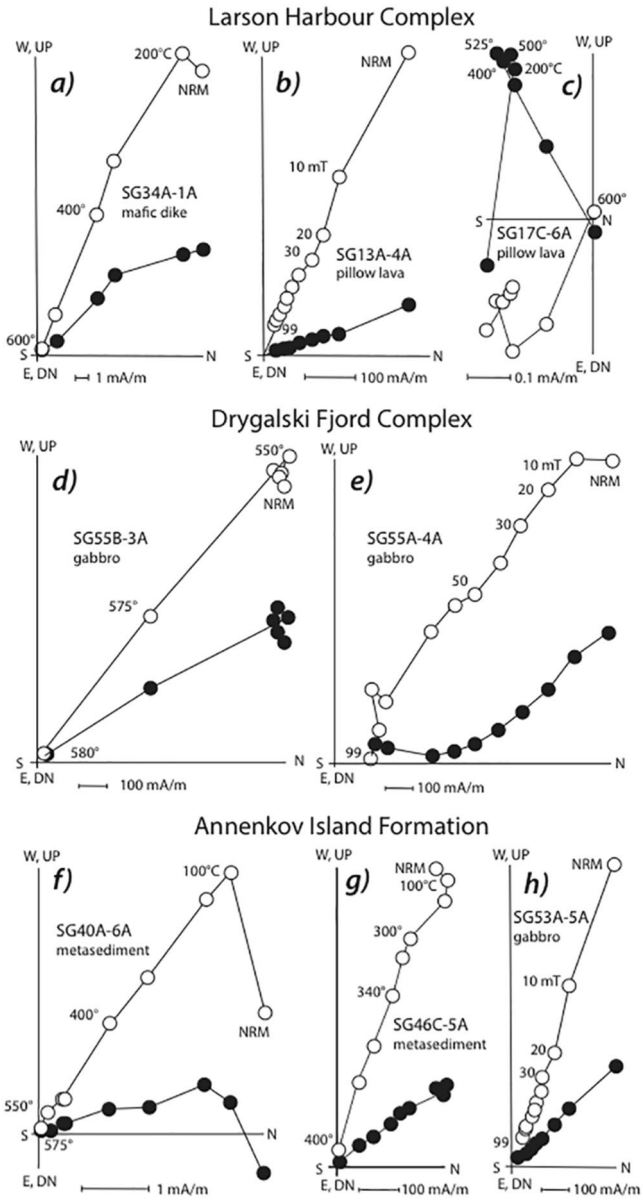

Figure 5. Vector end-point demagnetization diagrams of NRM of specimens from the Larsen Harbour Complex (a–c), Drygalksi Fjord Complex (d), (e) and the Annenkov Island Formation (f–h). Open/closed circles represent projections in the vertical/horizontal plane. Demagnetization levels in increments of mT for AF, and °C for thermal. All diagrams are plotted in geographic coordinates.

4.2.3. Annenkov Island Formation

Natural remanent intensities in the Annenkov Island Formation vary between 0.01 and 1 A/m. Thermal demagnetization proved effective revealing components in the metasediments of the Lower Tuff Member and the associated pillow lava. After the removal of spurious low unblocking temperature magnetizations, further thermal demagnetization defines two distinct categories based upon unblocking temperature range: (a) a moderate unblocking temperature group whose NRMs decay progressively to 575°C, most probably indicating magnetite (Figure 5f); and (2) a low unblocking temperature group which exhibits a dramatic intensity decrease between 360 and 400°C and whose magnetic carrier may be maghemite (Figure 5g). Nevertheless, the demagnetization trajectories consistently define a direction situated in the northwest quadrant with moderately steep negative inclination.

Thermal demagnetization of the gabbros in the most northeasterly island in the Pickersgill chain reveals a component with a very discrete spectrum of unblocking temperatures between 575 and 600°C. AF demagnetization provides a more continuous incremental decrease in NRM toward the origin and defines a univectoral component consistent with the dominant direction thus far determined, northwesterly with steep negative inclination (Figure 5h). Finally, the NRM of the diorites sampled on the most southwesterly island in the Pickersgill chain (sites SG51A and SG51B) were virtually unaffected by AF demagnetization to l00 mT. Thermal demagnetization to 650°C revealed no discernible components on vector endpoint diagrams and on this basis, this site was excluded from further analysis.

Site mean directions in geographic coordinates for the seven (of nine) accepted sites from the Annenkov Island Group are listed in Table 1 and plotted in Figure 6c, where they are grouped in the northwest quadrant with steep negative inclination (D/I = 331.1°/−62.9°, a95 = 7.8°). Four sites in the metasediments of the Lower Tuff Member and the site in a pillow lava provided structural control of small variability in bedding attitude and will be discussed below in the context of an overall differential tilt test.

4.3. Interpretation of Results

Of the total of 28 sites sampled from the Larsen Harbour Complex, the Drygalski Fjord Complex, and the Annenkov Island Formation, 21 sites were deemed to provide acceptable coherent magnetizations (precision parameter, k, typically greater than 50; Table 1). Locality-mean directions in geographic coordinates are well-grouped in the northwest quadrant and are of moderate to steep inclination (Figure 6d) with a mean (D/I = 328.5°/−62.1°, a95 = 3.5°, k = 86). Although the characteristic direction at all 21 sites is of normal polarity, the mean direction is significantly different mainly in declination than the present-day field direction (D/I = −7.4°/−53.8°) or the time-averaged geocentric axial dipole field direction (D/I = 0°/−70.4°).

Six of the sites (one from the Larsen Harbour Complex, five from the Annenkov Island Formation) have structural control of paleohorizontal and allow a differential tilt test to help constrain the age of magnetization (Table 2). Following correction for bedding tilt for the 6 sites with structural control, directions are seen to disperse (k_g/k_b = 2.18; Figures 6e and 6f), even though the change in precision parameter, k, is not significant at the 95% confidence level (k_g/k_b = 2.97 required for n = 6; McElhinny (1964)). The lack of a statistically diagnostic result is related to the relatively small differences in structural attitudes and the small number of sites with structural control, circumstances that are not encouraging in seeking a test in the hopes of obtaining a more statistically significant

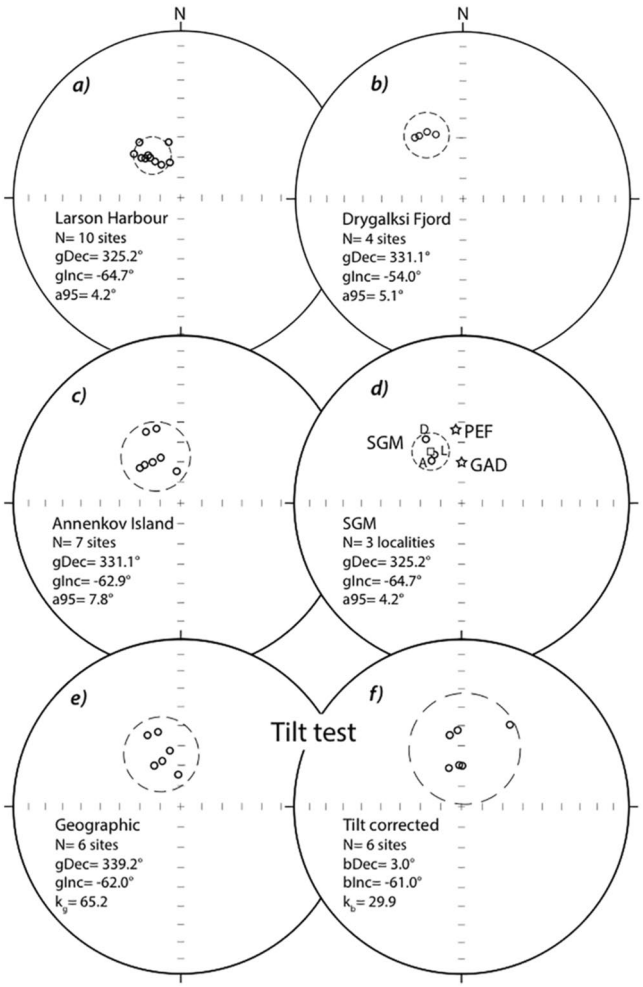

Figure 6. Equal area projections of mean directions (all on upper hemisphere) from (a) Larsen Harbour Complex sites, (b) Drygalski Fjord Complex sites, (c) Annenkov Island Formation sites, (d) the three sampling localities labeled D (Drygalski Fjord), L (Larsen Harbour) and L (Annenkov) with mean as open square and open stars as present Earth's field (PEF) and geocentric axial dipole (GAD) field. Differential tilt test for six sites from Larsen Harbour and Annenkov Island with structural control of paleohorizontal are shown in geographic (e) and tilt-corrected (f) coordinates. Dashed circle in each panel is circle of 95% confidence about the mean direction.

outcome. Nonetheless, other aspects of the paleomagnetic signature also point to a secondary origin for the magnetizations.

The consistency of directions is most striking when viewed in the context of the spectrum of samples collected from South Georgia. As previously noted, samples encompass a wide range of lithologies, covering a broad extent of geologic time. The layered gabbros of the Drygalski Fjord Complex have been dated as Early to Middle Jurassic (Tanner & Rex, 1979). The Larsen Harbour Complex spans the Late Jurassic through Early Cretaceous (Mukasa & Dalziel, 1996; Storey et al., 1977; Tanner & Rex, 1979) while paleontological evidence from the Lower Tuff Member of the Annenkov Island Formation indicates a Neocomian to Aptian age (Pettigrew, 1981). The dominance of a very similar direction of magnetization of predominantly normal polarity in samples spanning approximately 120 million years, a time interval that includes frequent field reversals in the Jurassic and Early Cretaceous (Gee & Kent, 2007; Gradstein et al., 2012; Figure 4), argues in favor of a secondary magnetization. The overall high consistency of the directions (circle of 95% confidence of only 3.5° for 21 site-means from widely distributed sites; Table 1) also argues against differential rotations about local vertical and horizontal axes since the time of acquisition of the ancient secondary magnetization. Gross tilting of the entire SGM subsequent to acquisition of the magnetization is of course a theoretical possibility that cannot be excluded by the paleomagnetic data. However, despite thermochronologic evidence of late Eocene or younger burial and subsequent tectonic uplift associated with collision with the Northeast Georgia Rise (Figure 1; Carter et al., 2014; Dalziel et al., 2021) there is no evidence of this. The low plunge of the Andean folds in the turbiditic strata is comparable to that in the equivalent formations in Tierra del Fuego and the bathymetry of the continental shelf is homogeneous around the island (Curtis, 2011; Fretwell et al., 2009).

Given that the magnetization is most probably secondary, the oldest age of acquisition is Neocomian/Aptian insofar as the youngest strata sampled exhibiting this direction is in the Lower Tuff Member (Figure 4). As frequently is the case with secondary magnetizations, the determination of the youngest age of acquisition is less directly established. Pertinent to this issue is the mid- to Late Cretaceous compression associated with the closure and inversion of the Rocas Verdes marginal basin. No significant geologic event younger than 80–90 Ma is documented by field relations or subsurface geology which might have generated the hydrothermal conditions conducive to remagnetization of the rocks sampled from the South Georgia block (Dalziel et al., 2021). A suggested mid- to Late Cretaceous age of magnetization would also be consistent with the dominance of normal polarity exhibited by South Georgia sites and the extended period of normal polarity during the Cretaceous Quiet Zone or Long Normal (121–184 Ma; Gee & Kent, 2007; Gradstein et al., 2012; Figure 4). Therefore, it is most probable that the secondary magnetization was acquired in the mid- to Late Cretaceous, no older than approximately 100 Ma and perhaps as young as the age of the ~81 Ma emplacement of the monzodioritic pluton of the Pickersgill Islands, but certainly not in the present field direction. Unfortunately, the samples collected from South Georgia were lost since the time of the paleomagnetic measurements and thus more detailed petrographic and rock magnetic analyses are unavailable to further constrain the origin of the magnetizations. Nonetheless, the moderate coercivities and unblocking temperatures ranging to less than 600°C (Figure 6) point to magnetite as the principal carrier of the stable component of NRM in these rock units.

The (north) pole position for the 21 site-mean directions in geographic coordinates expressed as virtual geomagnetic poles (VGPs) to account for differences in site locations falls at 67.2°N 248.2°E (A95 = 4.7°; Table 1). Virtually all recently compiled composite or global apparent polar wander (APW) paths show that South America

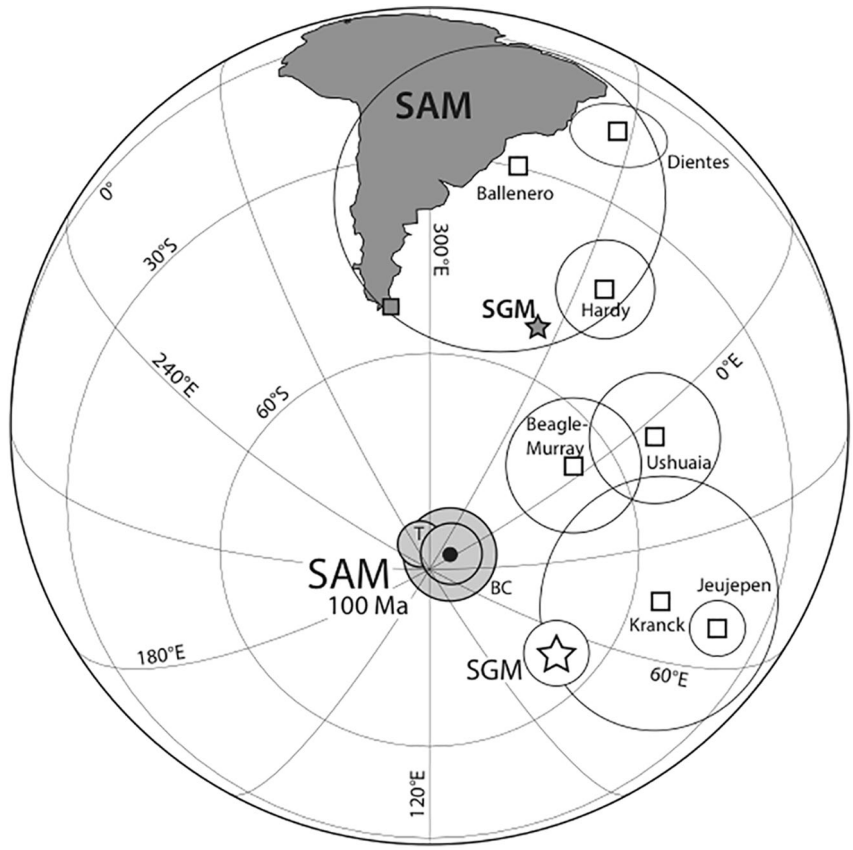

Figure 7. Paleomagnetic south pole for characteristic (albeit secondary) magnetization (open star labeled SGM; Tables 1 and 3) for South Georgia microcontinent (shaded star labeled SGM) compared to global composite mean 100 Ma pole (filled circle with circle of 95% confidence from Kent and Irving (2010) and Kent and Muttoni (2013), compared to 100 Ma poles from Besse and Courtillot (2003) labeled BC and from Torsvik et al. (2012) labeled L) projected into South America (SAM) coordinates shown in its present position. Open squares are published poles from rock units in southernmost South America (gray-filled square) with attributed ages in 75–125 Ma time window (Table 3). All poles shown with circles of 95% confidence.

has been close to its present position with respect to the geographic axis since at least 100 Ma. For example, the 100 Ma (south) pole for South America is at 86.0°S 358.1°E A95 = 4.4° in Kent and Muttoni (2013) and Kent and Irving (2010), 85.7°S 284.7°E A95 = 3.3° in Torsvik et al. (2012), and 86.7°S 357.9°E A95 = 6.7° in Besse and Courtillot (2003). The South Georgia (south) pole we derived (67.2°S 68.2°E A95 = 4.7°) is thus discordant with any robust mean reference pole for South America since at least 100 Ma (Figure 7).

The discordance of the South Georgia paleopole can be resolved into components of rotation (R) and flattening (F), and their 95% confidence limits, using the method and definitions of Beck (1980). The expected direction for the SGM using the 100 Ma pole from Kent and Muttoni (2013) is D\I = 355.7°\−72.6°. From the observed and expected 100 Ma directions, we calculate R = −27.2 ± 11.2° and F = −10.5° ± 4.5 (Table 3). Both the rotation, R, and flattening, F, are significant at 95% confidence. The discordance with the reference pole at 100 Ma thus includes a 27.2° counterclockwise rotation about a local vertical axis and a shallowing of 10.5° in the vertical component due to either northward tilting or movement toward a higher southerly latitude. Northward tilting would be consistent with uplift of the arc/batholith along the Pacific margin (e.g., Carter et al., 2014).

5. Discussion

As described above, South Georgia and the southernmost Andes have comparable tectonostratigraphic units of Late Jurassic-early Late Cretaceous age which developed as a consequence of continental rifting and back arc extension to form an island arc/marginal basin system. Beyond the lithologic and chronologic correspondence of

Table 3
Tectonic Rotations Inferred From Paleomagnetic Results From Rocas Verde Rock Units in Fuegian Andes and South Georgia of Late Cretaceous Age

Unit, Age	sLat (°S)	sLon (°W)	gDec (°)	gInc (°)	a95 (°)	R ± ΔR (°)	F ± ΔF (°)	pLat (°S)	pLon (°E)	A95 (°)	Ref.
South Georgia											
SGM, 80–200 Ma	54.70	36.30	328.5	−62.1	3.5	−27.2 ± 11.2	−10.5 ± 4.5	67.2	68.2	4.7	1
SGM', 80–200 Ma	56	60						66.3	48.9	4.7	1
Fuegian Andes, North of Beagle Channel											
Jeujepen, ~72 Ma	54.58	67.23	314.5	−33.6	4.5	−38.9 ± 9.9	−37.9 ± 5.3	40.0	50.7	4.0	2
Kranck, ~95 Ma	54.55	68.13	322.9	−51.8	16.5	−30.5 ± 28.5	−19.7 ± 16.7	55.8	47.0	19.0	2
Ushuaia, ~75 Ma	54.84	68.30	303.5	−66.9	6.9	−49.9 ± 19.8	−4.6 ± 7.4	55.9	6.7	9.4	2
Beagle-Murray, 82–89 Ma	54.92	68.27	316.8	−72.9	4.6	−36.6 ± 17.8	−1.4 ± 5.4	66.4	355.4	7.9	3
Fuegian Andes, South of Beagle Channel											
Dientes Navarino, 100–115	55.00	67.69	258.8	−73.2	9.7	−94.6 ± 36.6	−1.7 ± 10.1	40.1	333.8	16.4	3
Ballenero-Obrien, 100–125	55.93	70.52	225.7	−69.9	18.6	−126.8 ± 54.7	2.1 ± 15.0	25.9	317.5	29.8	3
Hardy, 100–115 Ma	55.43	68.11	265.8	−72.6	4.2	−87.5 ± 16.4	0.6 ± 5.0	42.6	337.8	7.1	4

Note. Paleomagnetic results from South Georgia microcontinent (SGM in present location, SGM' in a possible reconstructed position) compared to selected rock units in southernmost Andes with attributed ages of magnetization similarly between 75 and 125 Ma in Cretaceous Long Normal. Each rock unit and its estimated age is listed with a nominal site latitude (sLat) and site longitude (sLon) and a mean magnetization of declination (gDec) and inclination (gInc) in geographic coordinates with circle of 95% confidence (a95). R ± ΔR and F ± ΔF are net rotations about vertical (negative for counterclockwise) and E-W horizontal (positive for northward) axes with 95% uncertainties with respect to expected declination and inclination for 100 Ma global mean paleomagnetic north pole of Kent and Muttoni (2013) in South America coordinates (86.0°N 178.1°E, with A95 = 4.4° from Kent and Irving (2010)) projected to the sampling locations. Ref. are references to the primary results (gDec, gInc, a95). (1) This study; (2) Rapalini et al. (2016); (3) Poblete et al. (2016); (4) Cunningham et al. (1991).

these units, they also exhibit a similar metamorphic and structural zonation from the Pacific to the Atlantic in the southernmost Andes and from southwest to northeast on South Georgia. The metamorphic grade increases from zeolite facies outboard in the paleo-island arc thru prehnite-pumpellyite facies and local greenschist facies in the marginal basin assemblage inboard; deformational intensity likewise increases from gentle folding to the development of penetrative cleavage and tight asymmetric folds from the outer island arc to the inner marginal basin. These characteristics in common have been attributed to the cogenetic evolution of the southernmost Andes and South Georgia and suggest that the SGM is an eastward continuation of the Rocas Verdes marginal basin system that has been displaced relatively eastward from its paleo-tectonic position south of Burdwood Bank.

Paleomagnetic data reported here from South Georgia can be compared to published data from the Fuegian Andes, as recently summarized by Poblete et al. (2016) and Rapalini et al. (2016), to evaluate a shared tectonic association (Table 3). From Early Jurassic and Early Cretaceous sediments and interbedded volcanics in the southernmost Andes of Patagonia, Poblete et al. (2016) found normal polarity magnetizations of secondary origin similar in direction to mid-Cretaceous igneous intrusives, suggesting a widespread remagnetization event in the Cretaceous normal polarity superchron; the recovered paleomagnetic directions imply large (>90°) counterclockwise rotations in the same region as previously observed by Cunningham et al. (1991) (Table 3). Paleomagnetic results from magmatic units such as the Jeujepen pluton located inboard and to the north in the Fuegian Andes and with similar attributed ages of 75–125 Ma reported by Rapalini et al. (2016) often showed smaller counterclockwise rotations of ~30°–50° (Table 3), pointing to a geographic progression of larger rotations toward the more exterior parts of the Patagonian orocline as documented by Poblete et al. (2016) and others (Burns et al., 1980; Cunningham et al., 1991; Dalziel et al., 1973).

Our new paleomagnetic results from the SGM compare favorably with paleomagnetic data from the Fuegian Andes (Rapalini et al., 2016). Both sets of data indicate at least 30° counterclockwise tectonic rotation as well as flattening that could be interpreted as due to a variable northward component of tilting, for example, 10° for SGM compared to 38° in the case of the Jeujepen pluton but less than 5° for the Ushuaia dacite since the Late Cretaceous (Rapalini et al., 2016; Table 3). The corresponding (south) paleomagnetic pole positions for the SGM and the Fuegian Andes are scattered to the east of Cretaceous to Cenozoic reference poles that closely coincide with the present-day pole for South America (Figure 7). Both the significant counterclockwise rotation (−27.2 ± 11.2°)

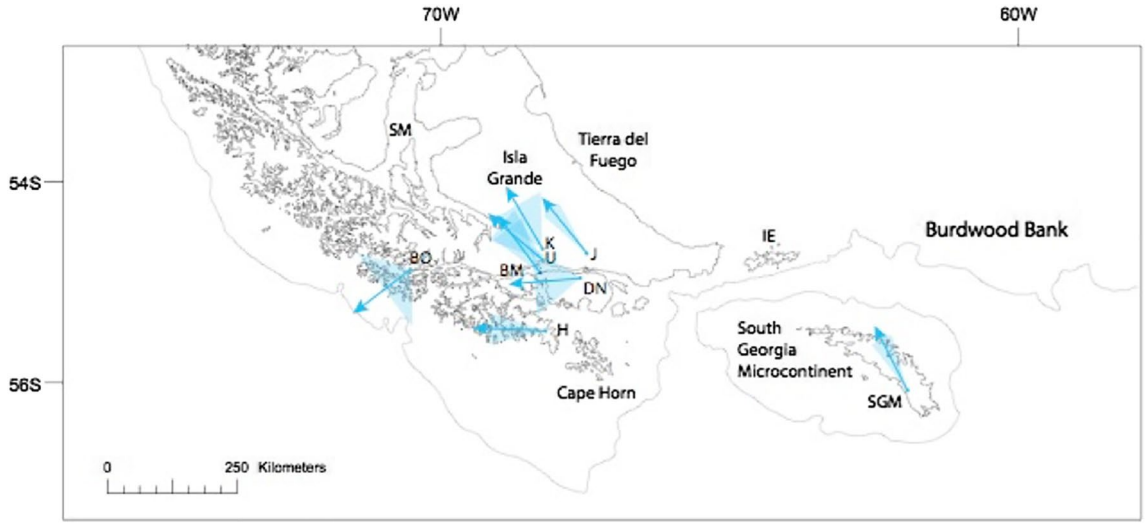

Figure 8. Paleogeographic model with South Georgia in its presumed pre-Late Cretaceous paleo-tectonic position (Dalziel et al., 2021) with arrow showing direction of measured declination with respect to paleomeridian at 100 Ma from South American apparent polar wander path with similar arrows for various sampling localities in southernmost South America including the Fuegian Andes, as labeled (see Table 3). Note that the present geographic orientation of the South Georgia microcontinent is maintained in the reconstruction. IE, Isla de lose Estados; SM, Strait of Magellan. Paleomagnetic sites (see Table 3): BO, Ballenero-Obrien C; BM, Beagle-Murray C; DN, Dientes de Navarino; H, Hardy; J, Jeujepen; K, Kranck; SGM, South Georgia microcontinent; U, Ushuaia.

and/tilting ($-10.5° \pm 4.5°$) implied by the SGM stable secondary magnetization are thus not inconsistent with the tectonic history inferred from the Fuegian Andes. It should be acknowledged that the paleomagnetic data do not in themselves preclude a paleoposition of the SGM much farther to the east of Cape Horn, adjacent to Maurice Ewing Bank (Figure 1), as argued by different plate kinematic scenarios for the Scotia Sea (Eagles, 2010b, 2016; Eagles & Eisermann, 2020); however, the correspondence of tectonostratiographic frameworks, termination of the Rocas Verdes basin at the Cape Horn escarpment and provenance of the Cretaceous sedimentary strata of the SGM, combined with the general similarities in the paleomagnetic signatures are strongly supportive of the traditional restored position of the SGM adjacent to the Fuegian Andes east of Cape Horn and south of Burdwood Bank (Dalziel & Elliot, 1971; Dalziel et al., 1975, 2021; Figure 8). The SGM, as part of the Fuegian Andes, apparently rotated ~30° counterclockwise with variable local northward tilting in the Late Cretaceous before the SGM rifted off and somehow was transported over 1,700 km along the North Scotia Ridge to its current position in the Scotia Sea, possibly in an "orogenic stream" (Redfield et al., 2007) escaping eastward during closure of the Rocas Verdes marginal basin (Dalziel et al., 2021).

Available evidence does not adequately constrain tectonic reconstructions of the Scotia Sea prior to 28 Ma due to the absence of older sea floor and unresolved displacement along the North and South Scotia Ridge although tenuous reconstructions extending to 40 Ma have been proposed (Barker & Hill, 1981). A model for 30 Ma (Barker et al., 1991), for example, succeeds only in returning the SGM half the distance to its presumed pre-drift position east of Cape Horn and south of Burdwood Bank (Eagles, 2010a). The issue remains as to how and when the apparent counterclockwise rotation of the SGM occurred, either as a consequence of oroclinal bending during Late Cretaceous disruption and fragmentation of the southernmost Andean cordillera following marginal basin inversion, during tectonic transport of the SGM along the North Scotia Ridge toward its current location during the Cenozoic development of the Scotia plate, or less likely, as an artifact of an unrelated island-wide tectonic tilt episode. The close correspondence of local rotations for the SGM compared to those for the Fuegian Andes immediately adjacent to its favored original paleogeographic venue would argue for a common tectonic origin: block rotations and tilting related to oroclinal bending. This would leave little to no necessity for invoking rotation during later transport of the SGM during creation of the Scotia Sea. Parallelism of structural trends in Tierra del Fuego in a reconstruction with South Georgia in its present geographic orientation (Figure 8 and figure 12 of Dalziel et al. (2021)) support this conclusion. Unfortunately, there are no rocks younger than Late Cretaceous on South Georgia to further constrain tectonic motions. Hence the possibility of counterclockwise rotation related to sinistral strike-slip motion along the North Scotia Ridge that transported the SGM to its present location, while geologically unlikely, cannot be tested paleomagnetically.

Data Availability Statement

The conclusions of this manuscript are based on primary paleomagnetic data collected by the authors. Site and locality-level tabulations of the paleomagnetic data are openly available in Zenodo via DOI: https://doi.org/10.5281/zenodo.5894945.

Acknowledgments
The field and laboratory work were funded and supported logistically by the National Science Foundation Division (now Office) of Polar Programs through Grant No. DPP-8643441 to Ian W. D. Dalziel. Paleomagnetic data used to support conclusions of the study are listed in Tables 1–3 of the main text. The authors wish to thank Captain Ulrich Mueller and the crew of RV *Polar Duke* for their skill and dedication to the success of the field work under arduous austral winter conditions, as well as to all the science participants on the field expedition (Hannes Brueckner, Anne Grunow. Sam Mukasa, Karen Schmidt, and Richard Veit). Support for Paleomagnetic Laboratory facilities was bootlegged from various NSF grants to Dennis Kent. We are also grateful to Doris Lafferty for able assistance in the laboratory work. We thank *Tectonics* Editor Margaret Rusmore, Associate Editor Augusto Rapalini, Fernando Poblete and an anonymous reviewer for constructive criticisms and suggestions that allowed us to improve the manuscript.

References

Barker, P. F., Dalziel, I. W. D., & Storey, B. C. (1991). In R. J. Tingey (Ed.), *The geology of Antarctica* (pp. 215–248). Clarendon Press. Tectonic development of the Scotia arc region.

Barker, P. F., & Hill, I. A. (1981). Back-arc extension in the Scotia Sea. *Philosophical Transactions of the Royal Society A*, *300*, 249–262.

Beck, M. E. (1980). Paleomagnetic record of plate-margin tectonic processes along the western edge of North America. *Journal of Geophysical Research*, *85*, 7115–7131.

Besse, J., & Courtillot, V. (2003). Correction to ''Apparent and true polar wander and the geometry of the geomagnetic field over the last 200 Myr''. *Journal of Geophysical Research*, *108*, 2469. https://doi.org/10.1029/2003JB002684

Bruce, W. S. (1905). Bathymetric survey of the South Atlantic Ocean and Weddell Sea. *Scottish Geographical Magazine*, *21*, 402–412.

Bruhn, R. L., Stern, C. R., & De Wit, M. J. (1978). Field and geochemical data bearing on the development of a Mesozoic volcano-tectonic rift zone and back-arc basin in southernmost South America. *Earth and Planetary Science Letters*, *41*(1), 32–46.

Burns, K. L., Rickard, M. J., Belbin, L., & Chamalaun, F. (1980). Further palaeomagnetic confirmation of the Magallanes orocline. *Tectonophysics*, *63*(1), 75–90.

Calderón, M., Prades, C. F., Hervé, F., Avendaño, V., Fanning, C. M., Massonne, H. J., et al. (2013). Petrological vestiges of the Late Jurassic-Early Cretaceous transition from rift to back-arc basin in southernmost Chile: New age and geochemical data from the Capitán Aracena, Carlos III, and Tortuga ophiolitic complexes. *Geochemical Journal*, *47*(2), 201–217.

Carey, S. W. (1955). The orocline concept in geotectonics. *Papers and Proceedings of the Royal Society of Tasmania*, *89*, 255–288.

Carter, A., Curtis, M., & Schwanethal, J. (2014). Cenozoic tectonic history of the South Georgia microcontinent and potential as a barrier to Pacific-Atlantic through flow. *Geology*, *42*(4), 299–302.

Cunningham, W. D., Klepeis, K. A., Gose, W. A., & Dalziel, I. W. D. (1991). The Patagonian Orocline: New paleomagnetic data from the Andean magmatic arc in Tierra del Fuego, Chile. *Journal of Geophysical Research: Solid Earth*, *96*(B10), 16061–16067.

Curtis, M. L. (2011). *Geological map of South Georgia (1:250 000 scale)*. British Antarctic Survey.

Dalziel, I. W. D. (1986). Collision and cordilleran orogenesis: An Andean perspective. *Geological Society of London Special Publication*, *19*, 389–404.

Dalziel, I. W. D., Caminos, R., Palmer, K. F., Nullo, F., & Casanova, R. (1974). The southern extremity of the Andes: Geology of Isla de los Estados, Argentine Tierra del Fuego. *American Association of Petroleum Geologists Bulletin*, *58*, 2502–2512.

Dalziel, I. W. D., de Wit, M. J., & Palmer, K. F. (1974). Fossil marginal basin in the southern Andes. *Nature*, *250*, 291–294.

Dalziel, I. W. D., Dott, R. H. J., Winn, R. D. J., & Bruhn, R. L. (1975). Tectonic relations of South Georgia Island to the southernmost Andes. The *Geological Society of America Bulletin*, *86*(7), 1034–1040.

Dalziel, I. W. D., & Elliot, D. H. (1971). Evolution of the Scotia Arc. *Nature*, *233*, 246–252.

Dalziel, I. W. D., Kligfield, R., Lowrie, W., & Opdyke, N. D. (1973). Paleomagnetic data from the southernmost Andes and the Antarctandes In D. H. Tarling, S. K. Runcorn (Eds.), *Implications of continental drift to the Earth Sciences*,1 (pp. 87–101). Academic Press.

Dalziel, I. W. D., Lawver, L. A., Norton, I. O., & Gahagan, L. M. (2013). The Scotia Arc: Genesis, evolution, global significance. *Annual Review of Earth and Planetary Sciences*, *41*(1), 767–793.

Dalziel, I. W. D., Lawver, L. A., Pearce, J. A., Barker, P. F., Hastie, A. R., Barfod, D. N., et al. (2013). A potential barrier to deep Antarctic circumpolar flow until the late Miocene? *Geology*, *41*(9), 947–950.

Dalziel, I. W. D., Macdonald, D. I. M., Stone, P., & Storey, B. C. (2021). South Georgia microcontinent: Displaced fragment of the southernmost Andes. *Earth Science Reviews*, *220*. https://doi.org/10.1016/j.earscirev.2021.103671

Dott, R. H., Winn, R. D., & Smith, C. H. L. (1982). Relationship of late Mesozoic and early Cenozoic sedimentation to the tectonic evolution of the southernmost Andes and Scotia Arc. In C. Craddock (Ed.), *Antarctic geoscience* (pp. 193–202). University of Wisconsin Press.

Eagles, G. (2010a). The age and origin of the central Scotia Sea. *Geophysical Journal International*, *183*(2), 587–600.

Eagles, G. (2010b). South Georgia and Gondwana's Pacific Margin: Lost in translation? *Journal of South American Earth Sciences*, *30*(2), 65–70.

Eagles, G. (2016). Plate kinematics of the Rocas Verdes basin and Patagonian orocline. *Gondwana Research*, *37*, 98–109.

Eagles, G., & Eisermann, H. (2020). The Skytrain plate and tectonic evolution of southwest Gondwana since Jurassic times. *Scientific Reports*, *10*(1), 19994. https://doi.org/10.1038/s41598-020-77070-6

Fisher, R. A. (1953). Dispersion on a sphere. *Proceedings of the Royal Society of London*, *A217*, 295–305.

Fretwell, P. T., Tate, A. J., Deen, T. J., & Belchier, M. (2009). Compilation of a new bathymetric dataset of South Georgia. *Antarctic Science*, *21*(2), 171–174.

Gee, J. S., & Kent, D. V. (2007). Source of oceanic magnetic anomalies and the geomagnetic polarity time scale. In M. Kono (Ed.), *Geomagnetism. Treatise on Geophysics* (Vol. 5, pp. 455–507). Elsevier. https://doi.org/10.1016/b978-044452748-6.00097-3

Goree, W. S., & Fuller, M. (1976). Magnetometers using RF-driven SQUIDs and their applications in rock magnetism and paleomagnetism. *Reviews of Geophysics and Space Physics*, *14*, 591–608.

Gradstein, F. M., Ogg, J. G., Schmitz, M. D., & Ogg, G. M. (Eds.). (2012). *The Geologic Time Scale 2012* (pp. 1–1144). Elsevier.

Hawkes, D. D. (1962). The structure of the Scotia Arc. *Geological Magazine*, *99*(1), 85–91.

Hervé, F., Pankhurst, R. J., Fanning, C. M., Calderón, M., & Yaxley, G. M. (2007). The South Patagonian batholith: 150 my of granite magmatism on a plate margin. *Lithos*, *97*, 373–394.

Horton, B. K., & Fuentes, F. (2016). Sedimentary record of plate coupling and decoupling during growth of the Andes. *Geology*, *44*, 647–650.

Katz, H. R. (1964). Some new concepts on geosynclinal development and mountain building at the southern end of South America. *Report of the 22nd International Geological Congress, New Delhi*, *4*, 241–256.

Katz, H. R. (1972). Plate tectonics – Orogenic belts in the southeast Pacific. *Nature*, *237*, 331.

Katz, H. R., & Watters, W. A. (1966). Geological investigation of the Yahgan Formation (Upper Mesozoic) and associated igneous rocks of Navarino Island, Southern Chile. *New Zealand Journal of Geology and Geophysics*, *9*, 323–359.

Kent, D. V., & Irving, E. (2010). Influence of inclination error in sedimentary rocks on the Triassic and Jurassic apparent polar wander path for North America and implications for Cordilleran tectonics. *Journal of Geophysical Research*, *115*, B10103.

Kent, D. V., & Muttoni, G. (2013). Modulation of Late Cretaceous and Cenozoic climate by variable drawdown of atmospheric pCO_2 from weathering of basaltic provinces on continents drifting through the equatorial humid belt. *Climate of the Past*, *9*, 525–546.

Kirschvink, J. L. (1980). The least-squares line and plane and the analysis of palaeomagnetic data. *Geophysical Journal of the Royal Astronomical Society*, *62*, 699–718.

Klepeis, K., Betka, P., Clarke, G., Fanning, M., Hervé, F., Rojas, L., et al. (2010). Continental underthrusting and obduction during the Cretaceous closure of the Rocas Verdes rift basin, Cordillera Darwin, Patagonian Andes. *Tectonics*, *29*(3). https://doi.org/10.1029/2009TC002610

Mair, B. F. (1983). The Larsen Harbour Formation and associated intrusive rocks of southern South Georgia. *British Antarctic Survey Bulletin*, *52*, 87–107.

Mair, B. F. (1987). Geology of South Georgia: VI. Larsen Harbour Formation. *British Antarctic Survey Scientific Reports*, *111*, 1–60.

Matthews, D. H. (1959). Aspects of the geology of the Scotia Arc. *Geological Magazine*, *96*(6), 425–441.

McElhinny, M. W. (1964). Statistical significance of the fold test in palaeomagnetism. *Geophysical Journal of the Royal Astronomical Society*, *8*, 338–340.

Molyneux, L. (1971). A complete result magnetometer for measuring the remanent magnetization of rocks. *Geophysical Journal of the Royal Astronomical Society*, *24*, 429–433.

Mukasa, S. B., & Dalziel, I. W. D. (1996). Southernmost Andes and South Georgia Island, North Scotia ridge: Zircon U-Pb and muscovite 40Ar/39Ar age constraints on tectonic evolution of southwestern Gondwanaland. *Journal of South American Earth Sciences*, *9*, 349–365.

Natland, M. L., Gonzalez, E. P., Cañon, A., & Ernst, M. (1974). A system of stages for correlation of Magallanes Basin sediments. *Geological Society of America Memoir*, *139*, 1–126.

Pettigrew, T. H. (1981). The geology of Annenkov Island. *British Antarctic Survey Bulletin*, *53*, 213–254.

Pettigrew, T. H., & Willey, L. T. (1975). Belemnite fragments from Annenkov Island. *British Antarctic Survey Bulletin*, *40*, 33–36.

Poblete, F., Roperch, P., Arriagada, C., Ruffet, G., Ramírez de Arellano, C., Hervé, F., & Poujol, M. (2016). Late Cretaceous–early Eocene counterclockwise rotation of the Fueguian Andes and evolution of the Patagonia–Antarctic Peninsula system. *Tectonophysics*, *668–669*, 15–34.

Poblete, F., Roperch, P., Hervé, F., Diraison, M., Espinoza, M., & Arriagada, C. (2014). The curved Magallanes fold and thrust belt: Tectonic insights from a paleomagnetic and anisotropy of magnetic susceptibility study. *Tectonics*, *33*(12), 2526–2551.

Rapalini, A. E. (2007). A paleomagnetic analysis of the Patagonian Orocline. *Geológica Acta*, *5*(4), 287–294.

Rapalini, A. E., Peroni, J., Luppo, T., Tassone, A., Elena Cerredo, M., Esteban, F., et al. (2016). Palaeomagnetism of Mesozoic magmatic bodies of the Fuegian Cordillera: Implications for the formation of the Patagonian Orocline. *Geological Society, London, Special Publications*, *425*(1), 65–80. https://doi.org/10.1144/sp425.3

Redfield, T. F., Scholl, D. W., Fitzgerald, P. G., & Beck, M. E. J. (2007). Escape tectonics and the evolution of Alaska; Past present and future. *Geology*, *35*, 1039–1042.

Stern, C. R., & de Wit, M. J. (2003). Rocas Verdes ophiolite, southernmost South America: Remnants of progressive stages of development of oceanic-type crust on a continental margin back-arc basin. *Geological Society, London, Special Publications*, *218*, 665–683. https://doi.org/10.1144/gsl.sp.2003.218.01.32

Stern, C. R., Mukasa, S. B., & Fuenzalida, P. (1992). Age and petrogenesis of the Sarmiento ophiolite complex of southern Chile. *Journal of South American Earth Sciences*, *6*, 97–104.

Stone, P., & Willey, L. E. (1973). Belemnite fragments from the Cumberland Bay type sediments of South Georgia. *British Antarctic Survey Bulletin*, *36*, 129–131.

Storey, B. C. (1983). The geology of South Georgia: V. Drygalski Fjord Complex. *British Antarctic Survey Scientific Reports*, *107*, 1–88.

Storey, B. C., & Mair, B. F. (1982). The composite floor of the Cretaceous back-arc basin of South Georgia. *Journal of the Geological Society, London*, *139*, 729–737. https://doi.org/10.1144/gsjgs.139.6.0729

Storey, B. C., Mair, B. F., & Bell, C. M. (1977). The occurrence of Mesozoic oceanic floor and ancient continental crust on South Georgia. *Geological Magazine*, *114*(3), 203–208.

Suarez, M., & Pettigrew, T. H. (1976). An Upper Mesozoic island-arc–back-arc system in the southern Andes and South Georgia. *Geological Magazine*, *113*, 305–328.

Tanner, P. W. G., & Rex, D. C. (1979). Timing of events in an Early Cretaceous island arc–marginal basin system on South Georgia. *Geological Magazine*, *116*(3), 167–179.

Tanner, P. W. G., Storey, B. C., & Macdonald, D. I. M. (1981). Geology of an Upper Jurrasic–Lower Cretaceous island-arc assemblage in Hauge Reef, the Pickersgill Islands and adjoining areas of South Georgia. *British Antarctic Survey Bulletin*, *53*, 77–117.

Torsvik, T. H., Van der Voo, R., Preeden, U., Mac Niocaill, C., Steinberger, B., Doubrovine, P. V., et al. (2012). Phanerozoic polar wander, palaeogeography and dynamics. *Earth-Science Reviews*, *114*, 325–368.

Zijderveld, J. D. A. (1967). A.C. demagnetization of rocks – Analysis of results. In D. W. Collinson, K. M. Creer, & S. K. Runcorn (Eds.), *Methods in paleomagnetism* (pp. 254–286). Elsevier.